Met Office Global Wave Model: Description and annual performance review, June 2022 to May 2023

Technical Report No. 655

October 2023

Breogán Gómez and Andrew Saulter

OFFICIAL

Document history

Version	Purpose	Date
0.1	Draft	21/09/2023
0.2	Revision	02/10/2023

Prepared by

Breogan Gomez, Science Manager – Ocean Forecasting R&D, 21/09/2023

Reviewed by

Andy Saulter, Science Strategic Head – Ocean Forecasting R&D, 02/10/2023

Authorised for issue by

Andy Saulter, Science Strategic Head – Ocean Forecasting R&D, 02/10/2023

Contents

1. Introduction

This is the first in a series of annual reports documenting the configuration and performance of the Met Office global wave forecast model. The configuration description covers model physics parameterisations, grid set-up and propagation, and the operational forecasting run cycle. Performance is assessed through verification of model against observations of overall sea-state.

Data from the global wave model are available through the Met Office Public Sector Information (PSI) re-use catalogue. The Met Office has also recently been nominated as a WMO Regional Specialised Meteorological Centre (RSMC) for global wave modelling. As part of this, some of the variables produced by our operational wave model will be made available to other WMO member organisations via the Global Data Processing and Forecasting System (GDPFS).

2. Model description

2.1 Codebase and physics parameterizations

The Met Office operational wave forecasting system is based on the WAVEWATCH III® third-generation spectral model (Tolman et al., 2014; WW3DG, 2023), version 7.12. A full description of Met Office systems for global and regional wave model forecasting can be found at Valiente et al. (2023)

The model resolves the evolution of the phase-averaged two-dimensional (frequency–direction) wave energy spectrum in time and space, conserving these changes in the presence of ocean currents through a description of wave action (Ardhuin et al., 2012, 2017). The total source term is defined by the combination of different physical processes that, in deep waters, can be simplified to a wind–wave interaction term that describes the transfer of momentum from the atmosphere to the ocean surface waves, a nonlinear wave–wave interaction term that describes energy transfers between waves of different frequencies and a dissipation term describing the loss of energy from the waves to the surrounding ocean and atmosphere(Valiente, Saulter, Edwards, et al., 2021). Additionally, the operational system includes a linear input term used to initialise the wave growth and parameterisations of shallow water processes (S_{brk}) and wave bottom interactions (S_{bf}).

The Met Office operational wave forecasting system uses the Ardhuin et al. (2010) ST4 package to parameterise wave growth (S_{in}) and dissipation via whitecapping (S_{diss}). For compatibility with Met Office Global Unified Model wind forecast data, a minor adjustment to the control of the input wind stress (BETAMAX namelist value set to 1.39) has been implemented. The model assumes a neutral atmospheric stability in these calculations. Additionally, a switch with linear wave growth (LN1; Cavaleri & Rizzoli, 1981) for lower winds is implemented (Valiente, Saulter, & Lewis, 2021) to enable the consistent spin-up of the model from calm conditions and a more accurate description of the initial wave growth.

The Discrete Interaction Approximation (DIA) package (NL1; Hasselmann et al., 1985) is used to resolve nonlinear wave–wave quadruplets interactions (S_{nl}) that enable downshifting of energy input in the upper tail of the wave spectrum into longer waves. As part of the shallow water physics, the Met Office wave model configurations include source terms to resolve depth-induced refraction, shoaling and breaking. Shallow water wave energy dissipation includes the surf-breaking parameterisation proposed by Battjes & Janssen (1978; DB1) and the JONSWAP (Joint North Sea Wave Project) bottom friction formulation (BT1; K. Hasselmann et al., 1973). Model spectral resolution uses 30 frequencies logarithmically spaced between 25 and 1.5 s (starting at 0.04118 Hz) and 36 directional bins that are linearly spaced.

2.2 Grid set-up and propagation scheme

Advection of wave energy through the model grid satisfies the wave dispersion relationship

for which wave energy at lower frequencies will travel more rapidly through the model grid than waves at high frequencies. All configurations of the Met Office operational forecasting system utilise the SMC grid (Li, 2012). One of the key features of this grid is that it allows higher-resolution cells in areas of interest (shallow water, coastal areas and islands), while maintaining a coarse resolution in the open ocean for computational efficiency. In the present system the variable resolution encompasses 25 km in open waters but is refined to 12 km and then 6 km around coastlines globally, with coastlines further resolved to 3 km around the UK. The areas surrounding the European Northwest Shelf are considered of special interest and the higher resolution areas are extended to cover open waters at 12 Km and shelf areas at 6 Km (Valiente et al., 2023). Grid cells are merged at high latitudes to relax the CFL restriction, and a fixed reference direction is used to define wave spectra in the polar region so that the whole Arctic Ocean could be included in the global domain.

The SMC grid retains quadrilateral cells, as in the standard latitude–longitude grid, so that simple finite difference schemes could be used for propagation calculations, with sub-time steps applied on different cell sizes for efficiency. The global wave model adopts a second-order upstream non-oscillatory (UNO) advection scheme (Li, 2008) for spatial propagation. The Garden Sprinkler Effect (GSE), caused by the discrete directional bins of the wave energy spectrum, is alleviated with a diffusion term similar to the PR2 option in WW3 model (Booij & Holthuijsen, 1987), plus an optional averaging scheme for further smoothing (WW3DG, 2023). The refraction-induced wave spectral rotation and the great circle turning are combined and calculated with a remapping scheme, which is not subject to the Courant–Friedrichs–Lewy (CFL) restriction but to a physical limit not exceeding the bathymetry gradient direction or a user-defined limit angle.

2.3 Operational run cycles

The model is forced using the Met Office Global operational coupled atmospheric-ocean model which runs at an effective resolution of 10 Km. Four model updates are provided with the 00Z and 12Z cycles running for 144 h and 06Z and 18Z for 66 h. The initialisation is provided by a wave model run from T-6 to T+0 forced with winds from an updated coupled atmospheric-ocean initialised from a data assimilation system with additional observations (Valiente et al., 2023).

3. Model performance

3.1. Baseline performance from June 2022 to May 2023

Baseline performance of the global wave model is described by comparing the model's initial condition (T+0) significant wave height fields to observations. The assessment uses two

different significant wave height observation datasets. WFVS is a dataset of in-situ observations maintained through the WMO Lead Centre for Wave Forecast Verification at ECMWF which include significant wave height, peak period and wind speed. Whilst the majority of these observations are sited away from the near-coastal zone, the data are predominantly representative of the northern hemisphere and approaches to land, rather than the open ocean. We also compare the model to a blend of satellite earth observations (JASON3, AltiKa SARAL and Sentinel 3a), which are representative of a wider range of open ocean areas due to the global coverage of the measurements and include significant wave height and wind speed. We focus our analysis on significant wave height but comments about the performance against other variables are included. Results are split by season and presented using scatter and quantile-quantile data.

3.1.1. WFVS

Model significant wave height performance is generally characterised by a small (order 0.1m) over-forecast (positive) bias for low wave heights (under 2m) and a similar order under-prediction (negative) bias for wave heights over 5m. The over-prediction bias dominates model performance statistics in the northern hemisphere summer (0.09m bias, 0.23m root mean squared error), when sea-states are relatively benign, and reduces to being neutral overall in the autumn and winter as storminess increases. Model errors are equivalent to between 20-30% of background variability in wave heights, with correlations at above the 95% level, representing a substantial skill improvement against climatology. Peak period and wind speed performance statistics (not shown) follow the behaviour of the wave height, although are somewhat poorer when compared to background variability. Higher waves are usually associated with larger peak periods. Similarly, large wind speeds yield larger waves and thus it is expected that RMSE and bias are related for the two variables. The peak period RMSE has a similar value for all periods of approx. 3 s, while the bias shows a seasonal variation, being positive between June and November (approx. 0.3 s) changing to a negative value (approx. -0.15 s) between December and May. The wind speed RMSE oscillates between 2-3m/s through the year and the bias shows near neutral values (between -0.7 and -0.18 m/s) except between December and February where the value lowers to -0.62 m/s. This is attributed to the overall larger winds occurring during this period in the Nother Hemisphere and is closely related to the negative bias also observed for the wave heights.

Global operational wave model – WFVS – 20220601 to 20220831

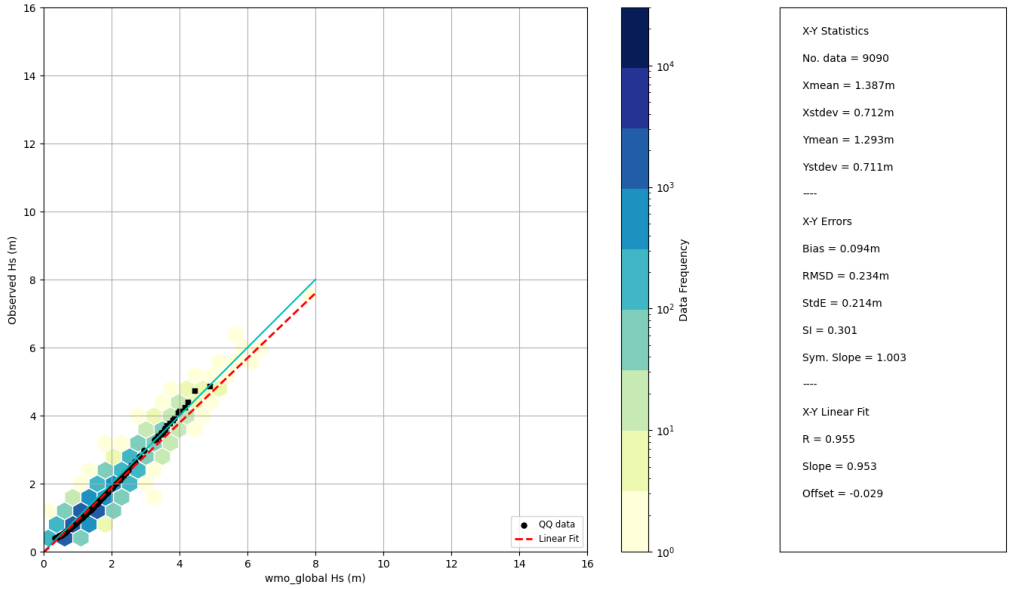

Figure 1 shows the distribution of model vs WFVS observed values for significant wave height between 01/06/2022 and 31/08/2022 (left). The data is represented in terms of density (hexagons) and quantile-quantile values in 1% intervals between 1% and 99% (black circles), 0.1% intervals between 99.1% and 99.9% (black squares), 0.01% intervals between 99.01% and 99.99% (black triangles), and 0.001% intervals between 99.991% and 99.999% (black crosses). Model and observed values are fitted to a linear regression (red) and a 45-degree line is plotted for reference (blue). The text box (right) presents standard statistical properties and verification scores.

Global operational wave model – WFVS – 20220901 to 20221130

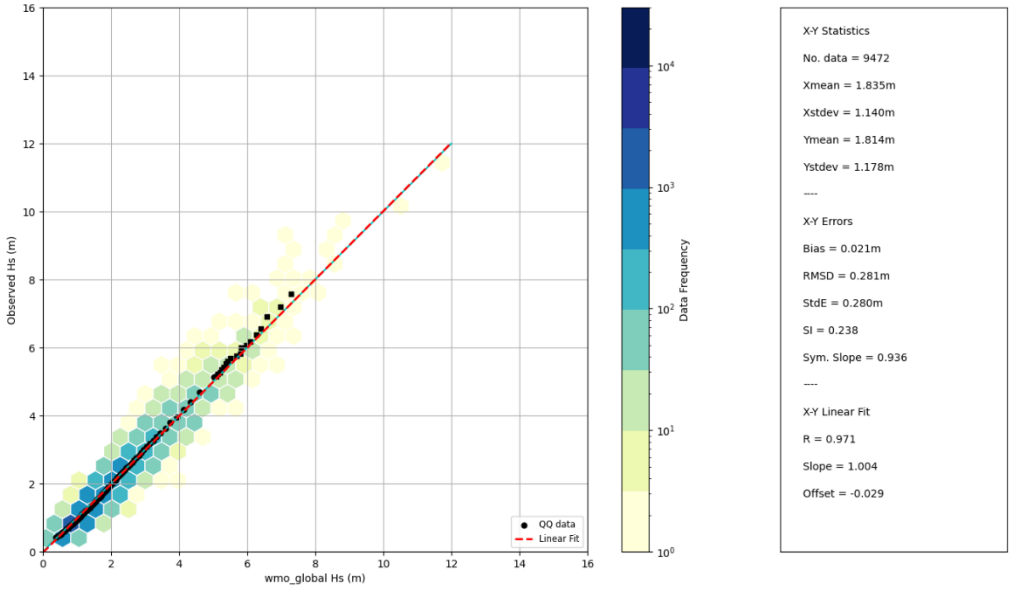

Figure 2 is as figure 1 but for the period between 01/09/2022 and 30/11/2022

Global operational wave model – WFVS – 20221201 to 20230228

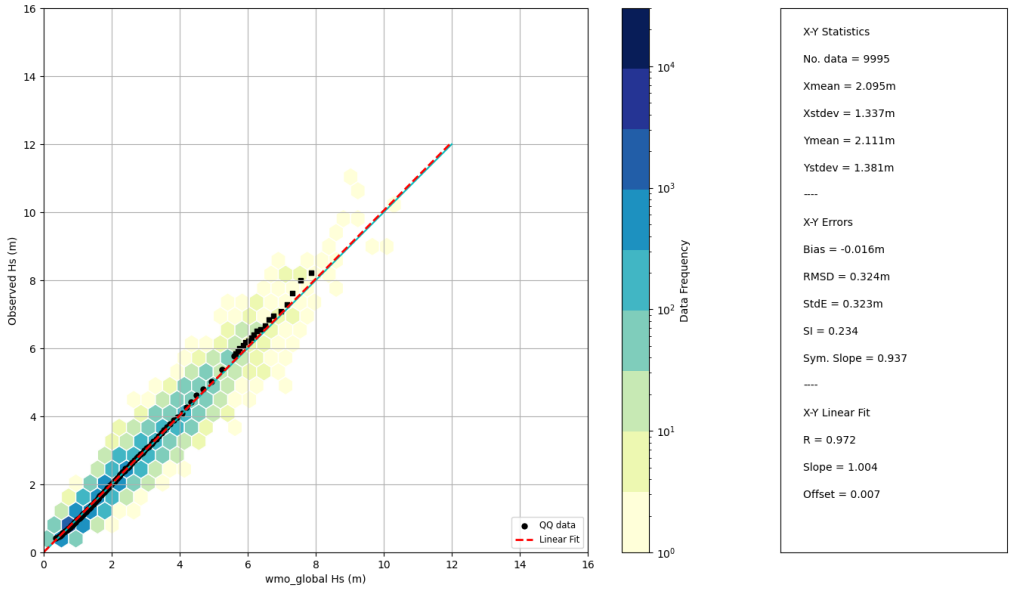

Figure 3 is as figure 1 but for the period between 01/12/2022 and 28/02/2023

Global operational wave model – WFVS – 20230301 to 20230531

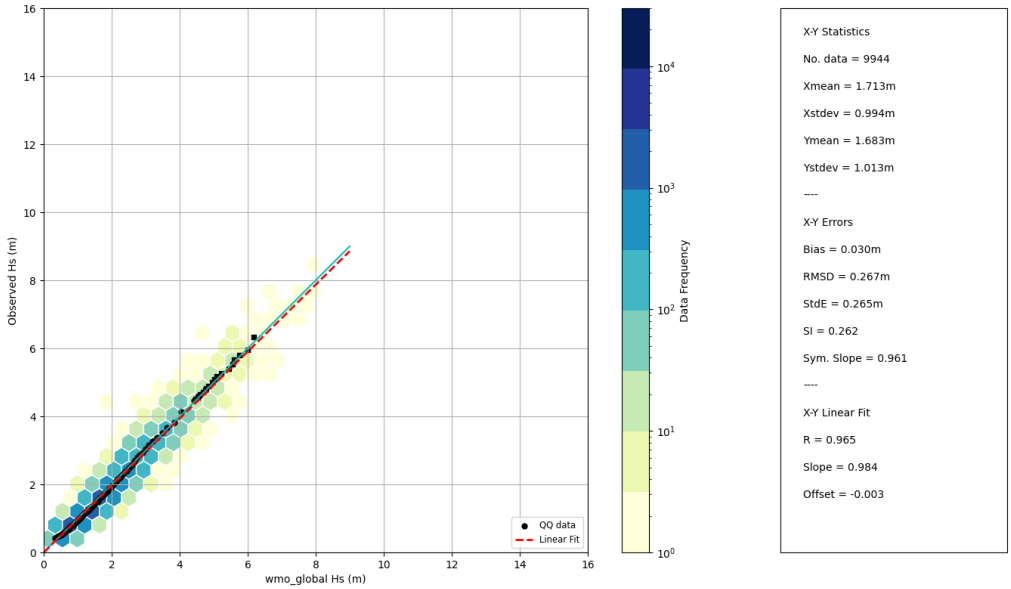

Figure 4 is as figure 1 but for the period between 01/03/2023 and 31/05/2023

3.1.2. Earth observations

Model significant wave height performance shows good agreement with observations up to weight heights of 8m, with an underprediction for higher values between 0.3 and 1 m. However, statistics for the most extreme values may be aliased due to low sampling. This is reflected in the overall bias, which is of the order of 0.1m, with some variation depending on the season. The root mean squared error is slight larger than for the WFVS (order of 0.4m) and this is a consequence of the overall larger wave highs measured in open seas. As with WFVS, model errors are equivalent to between 20-30% of background variability in wave heights, with correlations at above the 95% level, representing a substantial skill improvement against climatology. Wind speed stats (not shown) follow a similar behaviour to the wave height, with an overall bias of 0.2 m/s and a RMSE of 1.5 m/s. Compared to WFVS there is a smaller interannual variation in the stats due to the fact that this dataset provides global coverage and it is sampling different seasons in different hemispheres at the same time.

Global operational wave model – Earth observations – 20220601 to 20220831

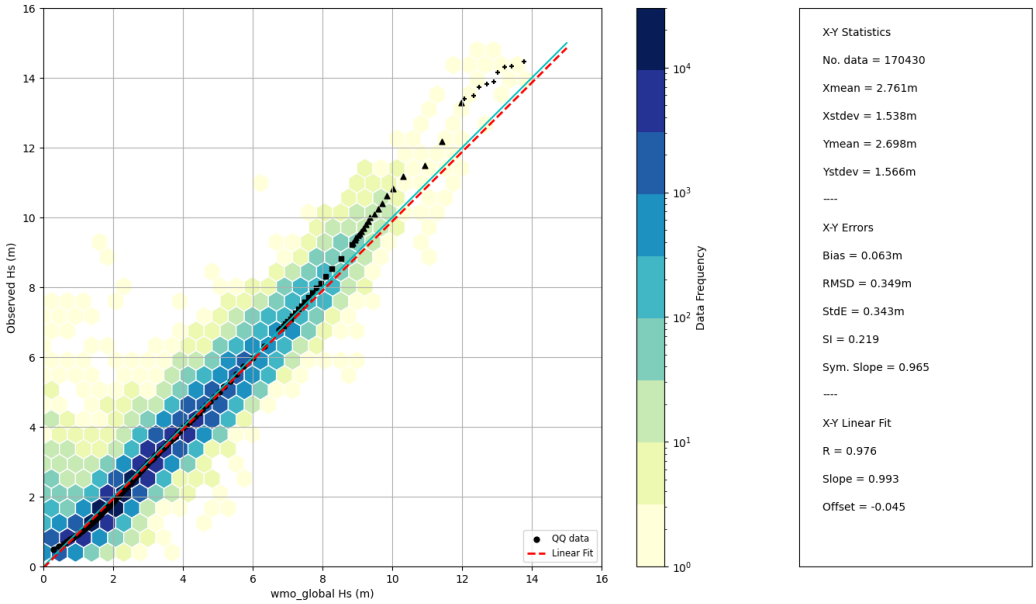

Figure 5 shows the distribution of model vs JASON3, AltiKa SARAL and Sentinel 3a observed values for significant wave height between 01/06/2022 and 31/08/2022 (left). The data is represented in terms of density (hexagons) and quantile-quantile values in 1% intervals between 1% and 99% (black circles), 0.1% intervals between 99.1% and 99.9% (black squares), 0.01% intervals between 99.01% and 99.99% (black triangles), and 0.001% intervals between 99.991% and 99.999% (black crosses). Model and observed values are fitted to a linear regression (red line) and a 45-degree line is plotted for reference (blue line). The text box (right) presents standard statistical properties and verification scores.

Global operational wave model – Earth observations – 20220901 to 20221130

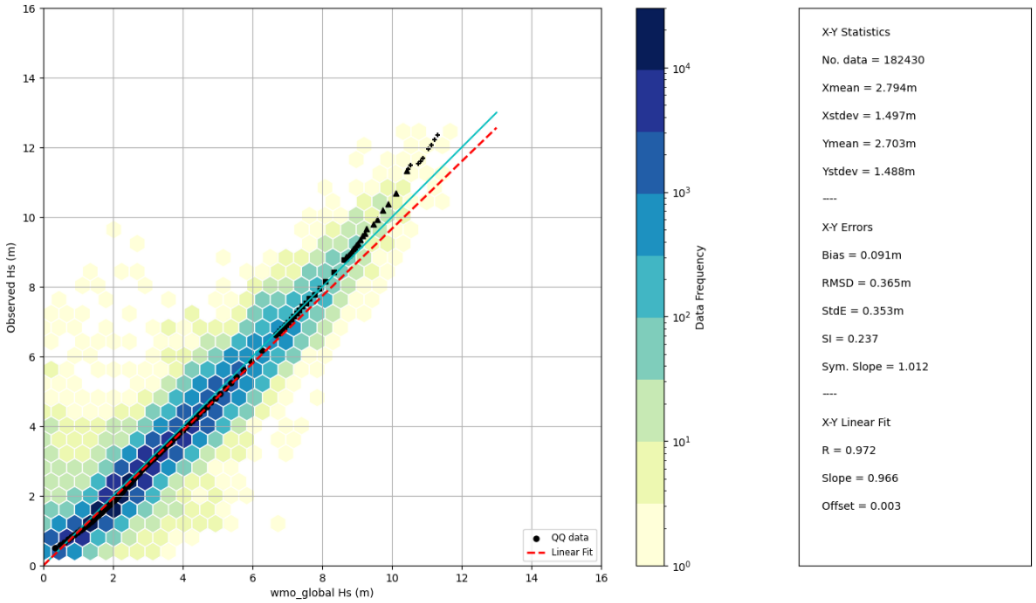

Figure 6 is as figure 5 but for the period between 01/09/2022 and 30/11/2022

Global operational wave model – Earth observations – 20221201 to 20230228

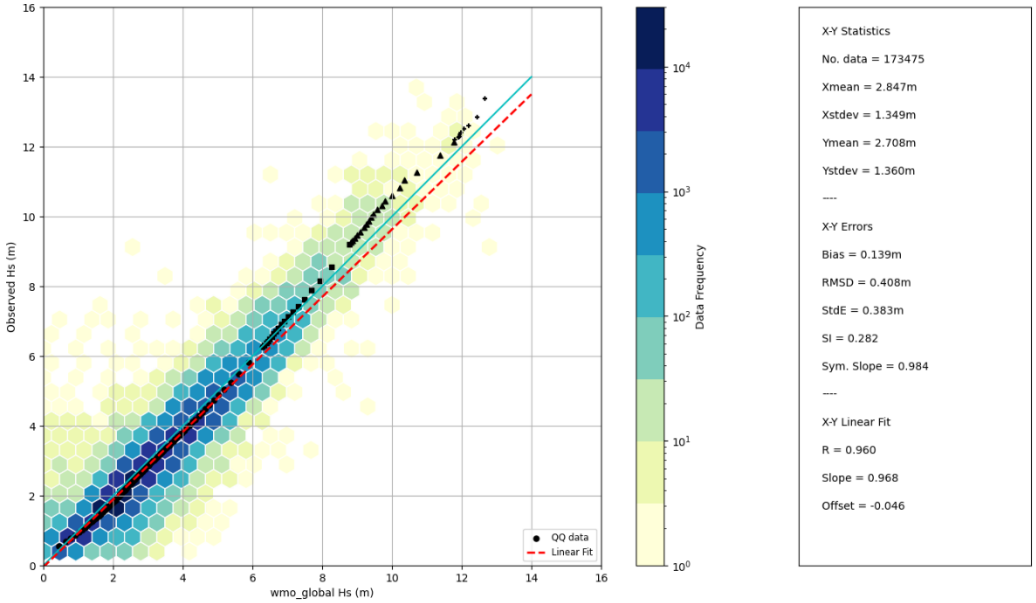

Figure 7 is as figure 5 but for the period between 01/12/2022 and 28/02/2023

Global operational wave model – Earth observations – 20230301 to 20220531

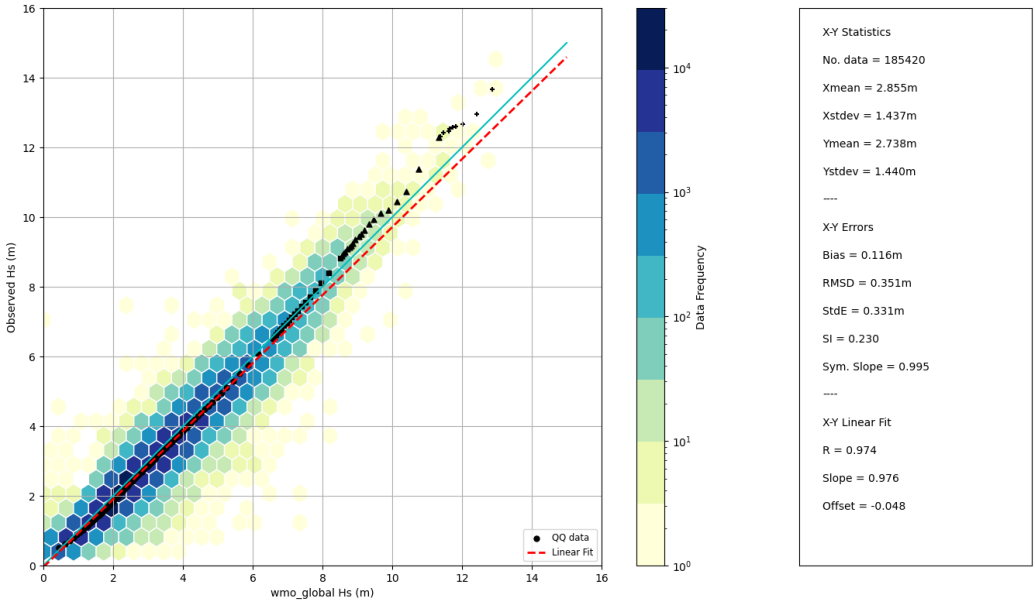

Figure 8 is as figure 5 but for the period between 01/03/2023 and 31/05/2023

3.2. Forecast Performance from June 2022 to May 2023

Forecast performance of the global wave model is described by comparing the model's significant wave height fields to observations and forecasts from other centres participating in the WMO Lead Centre for Wave Forecast Verification (LCWFV) global wave forecast intercomparison (Bidlot et al., 2002; Saetra & Bidlot, 2004). Plots are available from reports at https://confluence.ecmwf.int/display/WLW/Verification+results , with a subset reproduced here for convenience (figures 9 and 10). Model output is compared to the WFVS dataset and results are split into Northern Hemisphere Extratropics (NHE) and Tropical Ocean (TO). As indicated above, southern hemisphere is does not have enough coverage to provide meaningful stats and, therefore, results are not presented for this area. Verification for the European Northwest Shelf can be found in the LCWFV reports.

3.2.1. Significant wave height

Figure 9 shows seasonal performance comparisons of root mean squared error of significant wave height. Contrasted with background variability, the model remains skilful (versus a climatological estimate of wave height) at all forecast lead times out to 5-days ahead. RMSE is generally within 0.05m of the leading model (ECMWF), and generally the results sit within the top 5 global models. Performance in comparison to other systems is best in the autumn and winter, when sea-states are at their most variable.

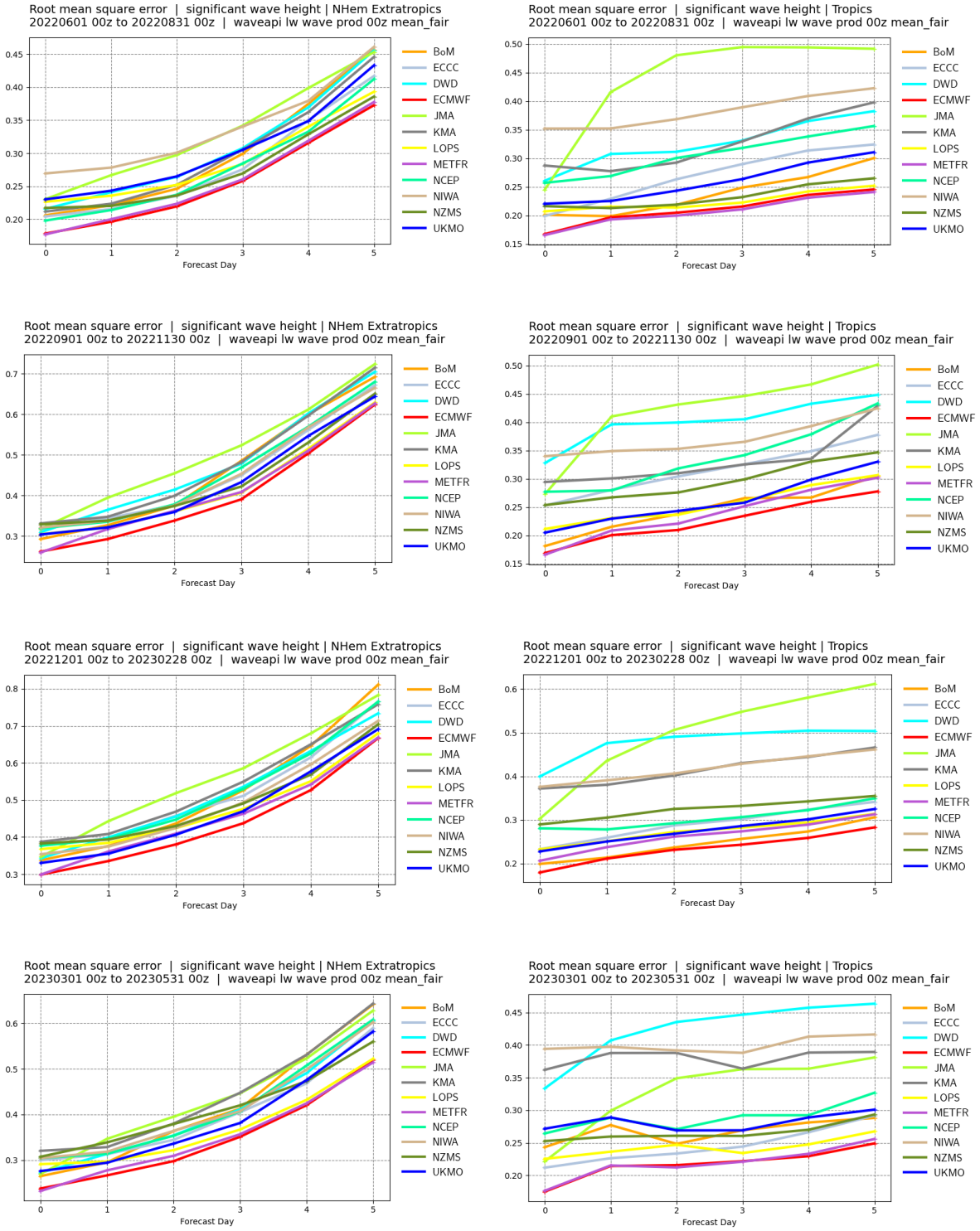

Figure 9 shows root mean squared error of various operational models against WFVS wave height for different lead times on the Northern Hemisphere (NHem, left) and the Tropics (right). Each row corresponds to the same periods of figures 1-4 and 5-8. Met Office is labelled as UKMO.

3.2.2. Peak period

Figure 10 shows seasonal performance comparisons of peak period against WFVS. The Met

Office RMSE shows consistent good performance across all lead times and periods on the NHem with respect to other centres, with values between 0.1 and 0.2 s above the leading centre. The RMSE increases as expected with the forecast day but still maintains a useful performance all the way up to day 5. Error is smaller for the winter period, when longer, more powerful swells are more common, and thus is more relevant to have accurate forecasts. The results for the Tropics show RMSE values around 2 s and a slightly larger distance to leading centre of 0.5 s with respect to the Northern Hemisphere. It is noteworthy that the RMSE value does not increase with lead time. We attribute this to both the smaller number of observations in this area, which result in a higher degree of sampling noise in the statistics, and the higher difficulty in accurately constraining peak period in tropical regions that are well away from major areas of storm generation (where the model wave physics will be more active).

4. Using Met Office wave data

4.1 Accessing global wave model data from the Met Office

For public and commercial users, Met Office global wave model data are available via the Met Office Public Sector Information re-use catalogue for NWP (Numerical Weather Prediction) model data:

- Full global coverage, at approximately 25km resolution (in mid-latitudes), is provided for 20 wave, wind-sea and swell parameters using 8 regional domains, updated for 00,06,12,18 UTC bulletins.
- A European area coverage, at approximately 6km resolution, is provided for 20 wave, wind-sea and swell parameters, updated for 00,06,12,18 UTC bulletins.

For members of the WMO, a full global coverage at approximately 25km (in mid-latitudes) will shortly be available for 4 overall sea-state parameters (significant wave height, peak and mean period and mean wave direction) plus the associated 10m wind zonal and meridional components. These data will be released via the Global Telecommunications System as part of the WMO's Global Data Processing and Forecasting System (GDPFS).

4.2 Interpreting the forecasts

Wave data in the Met Office global forecasts represent (approximately) an hourly sample of wave conditions. Individual waves vary in height, period and direction. Therefore, the parameters given in the forecast are statistics represent the sample of waves that may be experienced:

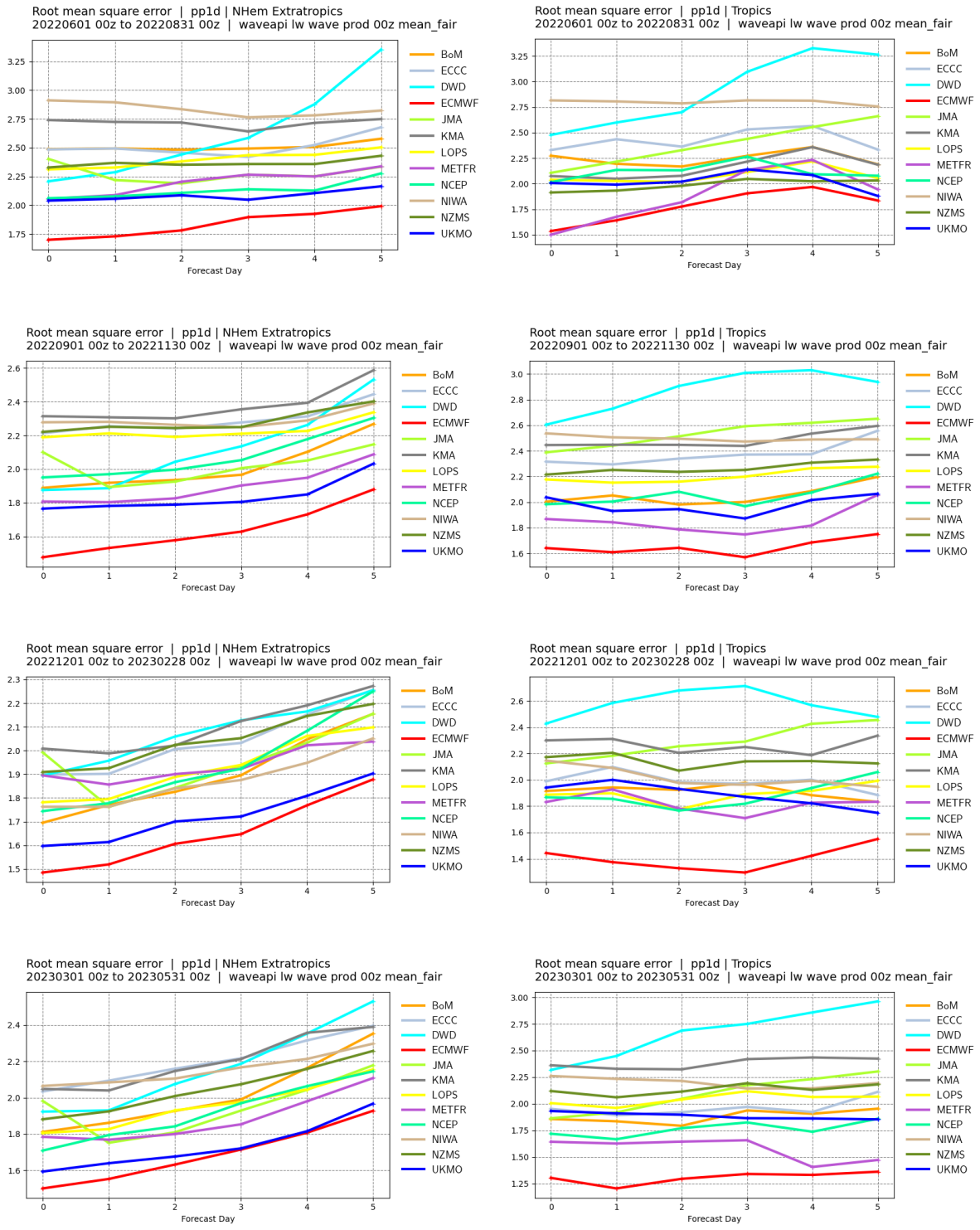

Figure 10 is as figure 9 but for wave peak period

- Significant wave height estimates the average height of the highest one-third of waves. Dependent on the definition used, maximum wave heights might usually be expected to be up to twice this value.

- Peak wave period indicates the period of the most energetic waves. Longer period waves will be more powerful and travel faster than shorter period waves. In complex seas comprising wind-sea and swell(s), peak period may vary rapidly with wind-shifts and changes in the dominant component of the overall sea-state.
- Mean zero-upcrossing period represents the period between successive wave faces (front part of the wave) and gives an indication of the frequency at which a static platform will encounter successive waves. For vessels this will alter depending on whether the vessel is travelling into (period shortens), away from (period lengthens) or perpendicular (no change) to the direction of wave travel. Mean zero-upcrossing period and significant wave height are often combined to provide a conservative estimate of wave steepness.
- Mean wave direction represents the average direction from which the waves travel. Meteorological (direction from) convention is used consistent with forecast wind. Where available, directional spread provides an indication of the variability in wave directions and, therefore, the degree to which wave energy in concentrated into a particular directional sector. Wind-seas are usually associated with a broad directional spread, leading to confused conditions, whilst mature swells have a narrow directional spread.

The wind-sea component of overall sea-state is estimated based on the relative speed of the waves compared to the forcing wind, with wind-sea energy combined over directions and periods where the wind is sufficiently strong to continue to modify the waves. Swell components are derived using a topographic analysis of the wave energy spectrum, with the forecasts defining up to three separate swell fields if required.

For more information on wave forecasting a interpretation of data, please see the WMO Guide to Wave Analysis and Forecasting.

4.3 Limitations on use

The Met Office global wave model is primarily designed for open waters wave prediction, based on a resolution that represents hourly conditions and fetches of 20-100km plus, and water depths of 20m plus. The data from the model may be useful in conditions outside of this design profile, but the data should be used with caution when:

- Close to the coast when the primary wind-sea component is generated by winds blowing offshore or along-shore.
- Close to the coast where complex topography and bathymetry may strongly influence sheltering and refraction of waves, particularly where waters are shallower than 20m.
- In regions with strong currents (e.g. Agulhas, Kuroshio, strongly tidal regions) – the global wave model does not presently include effects of currents on the waves.
- In highly convective weather, or scenarios where a storm centre may have a radius less than 100km.

References

Ardhuin, F., Gille, S. T., Menemenlis, D., Rocha, C. B., Rascle, N., Chapron, B., Gula, J., & Molemaker, J. (2017). Small-scale open ocean currents have large effects on wind wave heights. *Journal of Geophysical Research: Oceans*, *122*(6), 4500–4517. https://doi.org/https://doi.org/10.1002/2016JC012413

Ardhuin, F., Rogers, E., Babanin, A. V, Filipot, J.-F., Magne, R., Roland, A., van der Westhuysen, A., Queffeulou, P., Lefevre, J.-M., Aouf, L., & Collard, F. (2010). Semiempirical Dissipation Source Functions for Ocean Waves. Part I: Definition, Calibration, and Validation. *Journal of Physical Oceanography*, *40*(9), 1917–1941. https://doi.org/https://doi.org/10.1175/2010JPO4324.1

Ardhuin, F., Roland, A., Dumas, F., Bennis, A.-C., Sentchev, A., Forget, P., Wolf, J., Girard, F., Osuna, P., & Benoit, M. (2012). Numerical Wave Modeling in Conditions with Strong Currents: Dissipation, Refraction, and Relative Wind. *Journal of Physical Oceanography*, *42*(12), 2101–2120. https://doi.org/https://doi.org/10.1175/JPO-D-11-0220.1

Arun, C., Meixner, J., Campbell, T., Alves, J.-H., Ali, A., ardhuin, Accensi, M., Bunney, C., Masarik, M., Sikiric, M. D., Worthen, D., Sanchez, J. M. C., Roland, A., Gerheiser, K., Liu, Q., Hesser, T., Theurich, G., ukmo-nievesvaliente, Pouliot, B., … Ji, M. (2023). *WW3 Development Group (WW3DG): ukmo-waves/WW3: ukmo_ps45-1.1*. Zenodo. https://doi.org/10.5281/zenodo.7874843

Battjes, J., & Janssen, J. (1978). ENERGY LOSS AND SET-UP DUE TO BREAKING OF RANDOM WAVES. *Coastal Engineering Proceedings*, *1(16)*(32). https://doi.org/10.9753/icce.v16.32

Bidlot, J.-R., Holmes, D. J., Wittmann, P. A., Lalbeharry, R., & Chen, H. S. (2002). Intercomparison of the Performance of Operational Ocean Wave Forecasting Systems with Buoy Data. *Weather and Forecasting*, *17*(2), 287–310. https://doi.org/https://doi.org/10.1175/1520-0434(2002)017<0287:IOTPOO>2.0.CO;2

Booij, N., & Holthuijsen, L. H. (1987). Propagation of ocean waves in discrete spectral wave models. *Journal of Computational Physics*, *68*(2), 307–326. https://doi.org/https://doi.org/10.1016/0021-9991(87)90060-X

Cavaleri, L., & Rizzoli, P. M. (1981). Wind wave prediction in shallow water: Theory and applications. *Journal of Geophysical Research: Oceans*, *86*(C11), 10961–10973. https://doi.org/https://doi.org/10.1029/JC086iC11p10961

Hasselmann, K., Barnett, T. P., Bouws, E., Carlson, H., Cartwright, D. E., Enke, K., Ewing, J. A., Gienapp, H., Hasselmann, D. E., Kruseman, P., Meerburg, A., Müller, P., Olbers, D. J., Richter, K., Sell, W., & Walden, H. (1973). *Measurements of wind-wave growth and swell decay during the Joint North Sea Wave Project (JONSWAP)*. http://resolver.tudelft.nl/uuid:f204e188-13b9-49d8-a6dc-4fb7c20562fc

Hasselmann, S., Hasselman, K., Allender, J. H., & Barnett, T. P. (1985). Computations and

parameterizations of the nonlinear energy transfer in a gravity-wave spectrum, Part II: parameterizations of the nonlinear energy transfer for application in wave models. *J. Phys. Oceanogr*, *15*, 1378–1391.

Li, J.-G. (2008). Upstream Nonoscillatory Advection Schemes. *Monthly Weather Review*, *136*(12), 4709–4729. https://doi.org/https://doi.org/10.1175/2008MWR2451.1

Li, J.-G. (2012). Propagation of ocean surface waves on a spherical multiple-cell grid. *Journal of Computational Physics*, *231*(24), 8262–8277. https://doi.org/https://doi.org/10.1016/j.jcp.2012.08.007

Saetra, Ø., & Bidlot, J. R. (2004). Potential benefits of using probabilistic forecasts for waves and marine winds based on the ECMWF ensemble prediction system. *Weather and Forecasting*, *19*(4), 673–689. https://doi.org/10.1175/1520-0434(2004)019<0673:PBOUPF>2.0.CO;2

Tolman, H., Accensi, M., Alves, J.-H., Ardhuin, F., Bidlot, J., Booij, N., Bennis, A.-C., Campbell, T., Chalikov, D., Filipot, J.-F., Foreman, M., Janssen, P., Leckler, F., Li, J.-G., Chawla, A., Lind, K., Orzech, M., Padilla-Hernandez, R., Rogers, E., & Zieger, S. (2014). *User manual and system documentation of WAVEWATCH III version 4.18*.

Valiente, N. G., Saulter, A., Edwards, J. M., Lewis, H. W., Castillo Sanchez, J. M., Bruciaferri, D., Bunney, C., & Siddorn, J. (2021). The Impact of Wave Model Source Terms and Coupling Strategies to Rapidly Developing Waves across the North-West European Shelf during Extreme Events. *Journal of Marine Science and Engineering*, *9*(4). https://doi.org/10.3390/jmse9040403

Valiente, N. G., Saulter, A., Gomez, B., Bunney, C., Li, J. G., Palmer, T., & Pequignet, C. (2023). The Met Office operational wave forecasting system: the evolution of the regional and global models. *Geoscientific Model Development*, *16*(9), 2515–2538. https://doi.org/10.5194/gmd-16-2515-2023

Valiente, N. G., Saulter, A., & Lewis, H. W. (2021). *The effect of different levels of coupling in surface wind waves along the NWS during extreme events, Met Office Weather Science Report*. *January*, 1–38. https://digital.nmla.metoffice.gov.uk/IO_054d5518-86af-4a24-903d-fafa0d6a2695/

Met Office
FitzRoy Road
Exeter
Devon
EX1 3PB
United Kingdom